

# Size dependence of dielectric properties and structural metastability in ferroelectrics

L. Zhang<sup>a</sup>, W.L. Zhong, C.L. Wang, Y.P. Peng, and Y.G. Wang

Department of Physics, Shandong University, Jinan, 250100, P.R. China

Received 3 August 1998 and Received in final form 22 November 1998

**Abstract.** The size effect of the dielectric properties and the barrier height was investigated in the ferroelectric solid solution  $\text{Ba}_x\text{Sr}_{1-x}\text{TiO}_3$  system. The decrease of the grain size causes the suppression of the ferroelectricity, and the increase of the relaxation frequency. Barrier heights increase with increasing grain size. The result is analogous to magnetic phase transitions in nanocrystals and other solid-solid phase transitions in nanocrystals. It suggests a general rule that may be of use in the discovery of new metastable phases. An explanation of this phenomenon was given by an electric potential model that agrees well with the experimental results. For  $\text{Ba}_x\text{Sr}_{1-x}\text{TiO}_3$  system, the decrease of  $x$  causes the decrease of the barrier height.

**PACS.** 77.22.Gm Dielectric loss and relaxation – 77.80.Bh Phase transitions and Curie point – 77.80.-e Ferroelectricity and antiferroelectricity

## 1 Introduction

In order to expand the range of available ferroelectric materials, it is important to discover pathways that lead to metastable, high-energy structures. Sometimes, a high-energy form of a ferroelectric is observed to persist indefinitely at ambient conditions. A general understanding of what determines the energy barriers between crystal structures does not currently exist. However, the first-principles calculation has caused an increasing understanding of the ground state properties of ferroelectrics recently. First-principles LAPW calculations [1, 2] explained the decrease of the Curie temperature of  $\text{BaTiO}_3$  with hydrostatic pressure [3]. It indicated that the potential surface was strongly dependent on cell volume of  $\text{BaTiO}_3$  in eight-site potential model [4, 5], and the potential wells in cells would become much shallower as pressure was increased [1, 2]. Obviously, it is a very important result. Furthermore, the development of routine syntheses of nanocrystals creates the opportunity to study metastability as a function of a new variable, the size of the crystal. Such experiments may be analogous to studies of supercooling in liquid droplets [6, 7]. Nanosized ferroelectric particles have properties that are significantly different from those of the corresponding bulk materials. For example, in ferroelectric phase, they are single-domain particles and the polarization direction fluctuates spontaneously. Their dielectric relaxation frequency is given by

$$f_r = f_{r0} \exp\left(-\frac{h}{kT}\right)$$

<sup>a</sup> e-mail: xmliu@sdu.edu.cn

where  $f_{r0}$  is a constant,  $h$  is the energy barrier,  $k$  is the Boltzmann constant, and  $T$  is the temperature.

In this study we investigated the dielectric phenomena of  $\text{Ba}_x\text{Sr}_{1-x}\text{TiO}_3$  ( $x = 0.3, 0.5, 0.7$ ) ceramics of various grain size, and obtain the information on their relative barrier height. The solid solution  $\text{Ba}_x\text{Sr}_{1-x}\text{TiO}_3$  and its end member  $\text{BaTiO}_3$  both have perovskite structure. Similar to  $\text{BaTiO}_3$ ,  $\text{Ba}_x\text{Sr}_{1-x}\text{TiO}_3$  for high concentration  $x$  [8, 9] also has three phase transitions (trigonal-orthorhombic, orthorhombic-tetragonal, tetragonal-cubic). Our previous work [9, 10] showed that the variation of  $T_c$  in  $\text{Ba}_x\text{Sr}_{1-x}\text{TiO}_3$  was determined by changes in the cell volume. Furthermore, we found that the change of order and diffuseness of phase transition in  $\text{Ba}_x\text{Sr}_{1-x}\text{TiO}_3$  could be attributed to a cell volume effect. The mechanism of successive transitions of  $\text{Ba}_x\text{Sr}_{1-x}\text{TiO}_3$  should be similar to that of  $\text{BaTiO}_3$ . Thus  $\text{Ba}_x\text{Sr}_{1-x}\text{TiO}_3$  become a suitable system to study the size effect of the energy barrier of ferroelectrics systematically.

## 2 Experiment

The ultrafine  $\text{Ba}_x\text{Sr}_{1-x}\text{TiO}_3$  ( $x = 1, 0.7, 0.5, 0.3$ ) particles with high crystallinity were prepared by the sol-gel method [11]. The ceramics with different grain size were obtained by altering the firing conditions. The atmosphere during firing is air. For  $x = 0.7, 0.5$  and  $0.3$ , the grain sizes of the ultrafine particles as starting materials are 170 nm, 260 nm and 130 nm respectively. The work on the dielectric behavior of  $\text{BaTiO}_3$  ceramics was reported in reference [11].

**Table 1.** Grain size and density of  $\text{Ba}_x\text{Sr}_{1-x}\text{TiO}_3$  ceramics.

material	$\text{Ba}_{0.7}\text{Sr}_{0.3}\text{TiO}_3$					
grain size(nm)	200	220	260	370	1100	1860
density(%)	49	55	60	66	79	82
material	$\text{Ba}_{0.5}\text{Sr}_{0.5}\text{TiO}_3$					
grain size(nm)	330	375	600	860	1010	1610
density(%)	54	61	76	79	81	82
material	$\text{Ba}_{0.3}\text{Sr}_{0.7}\text{TiO}_3$					
grain size(nm)	230	475	1900	2970	-	-
density(%)	44	44	45	46	-	-

The dielectric properties of the samples were measured as a function of temperature using a HP 4192A impedance analyzer in the temperature range from 10 K to 400 K. They were also measured as a function of frequency using the HP 4192A impedance analyzer (10 Hz ~ 10 MHz) and a HP 4191A impedance analyzer (1 MHz ~ 1000 MHz).

The grain size, shape, and size distribution were studied by electron microscopy. Table 1 shows average grain size and density of  $\text{Ba}_x\text{Sr}_{1-x}\text{TiO}_3$  ceramics.

Some samples were chosen for stoichiometry analysis. The total stoichiometry was obtained by using a VRA-20 X-ray fluorescence spectrometer. The result showed that they had a standard stoichiometry of  $\text{Ba}_x\text{Sr}_{1-x}\text{TiO}_3$ . The surface composition of the  $\text{BaTiO}_3$  powder samples and ceramics samples was analyzed using a VG Scientific Escslab MK II X-ray photoelectron spectrometer. The measured surface ratio of Ba/Ti is between 0.98 and 1.05.

An X-ray-diffraction study at room temperature showed that all of the samples were single-phase perovskite solid solutions. For all of the samples, the (100) peak and (001) peak can not be distinguished from each other, and neither the (200) and (002) peak. The dielectric measurement showed that the  $T_c$  of the  $\text{Ba}_{0.7}\text{Sr}_{0.3}\text{TiO}_3$  samples with large grain size were above room temperature. Thus the structure of the large-grain  $\text{Ba}_{0.7}\text{Sr}_{0.3}\text{TiO}_3$  ceramics should be pseudo-cubic at room temperature. The other samples are cubic.

### 3 Results and discussion

Considering the porosity of the samples, the dielectric constant was calculated by taking the samples to be 0-3 composite of  $\text{Ba}_x\text{Sr}_{1-x}\text{TiO}_3$  particles and air [12]. A “0-3 composite” is a two-component composite in which one component is zero-dimensional (particles) and the other component is the three-dimensionally connected matrix. The porosity of the samples was calculated by comparing the measured density with the theoretical one.

We measured the temperature dependence of the dielectric constant  $\epsilon$  at 100 kHz for  $\text{Ba}_x\text{Sr}_{1-x}\text{TiO}_3$  ( $x = 0.7, 0.5, 0.3$ ) samples of different grain size. Figure 1 shows the temperature dependence of the dielectric constant of  $\text{Ba}_x\text{Sr}_{1-x}\text{TiO}_3$  ceramics. All these measurements were performed during the cooling cycle. With the decrease

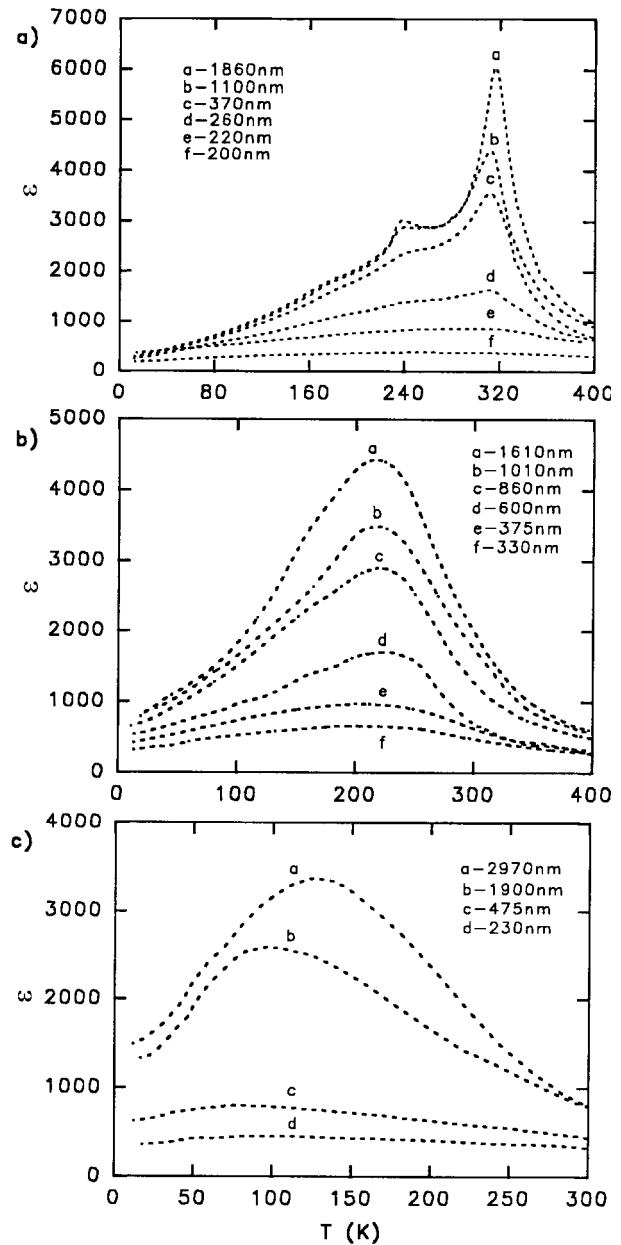


**Fig. 1.** The temperature dependence of the dielectric constant of the  $\text{Ba}_x\text{Sr}_{1-x}\text{TiO}_3$  with different mean grain sizes. (a)  $x = 0.7$ , (b)  $x = 0.5$ , (c)  $x = 0.3$ .

of grain size, the dielectric peaks of our samples become smaller and broader and eventually disappear. The ferroelectric  $T_c$  is identified as the temperature corresponding to the maximum value of the dielectric constant. Figure 2 shows the grain size dependence of  $T_c$  of the  $\text{Ba}_x\text{Sr}_{1-x}\text{TiO}_3$  ceramics. It is seen that the Curie temperature decreases with decreasing grain size. The dashed line drawn through the data points is the result obtained from an empirical equation [13–15]:

$$T_c(D) = T_c(\infty) - C/(D - D_s) \quad (\text{K}) \quad (1)$$

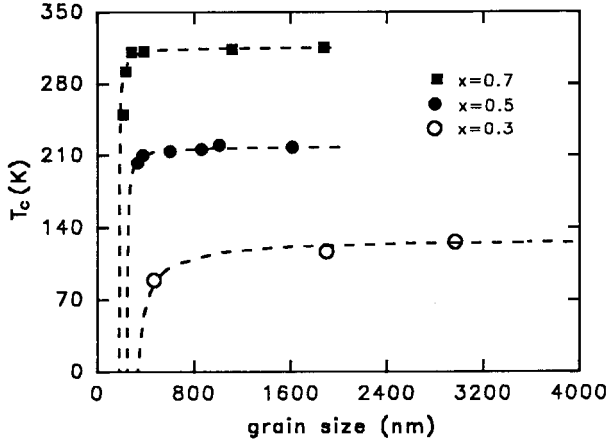


**Fig. 2.** Grain size dependence of  $T_c$  for  $\text{Ba}_x\text{Sr}_{1-x}\text{TiO}_3$  ceramics. The dashed line drawn through the data points is the result obtained from equation (1).

where  $C$  and  $D_s$  are two constants,  $D$  the grain size,  $T_c(\infty)$  the bulk Curie temperature. For  $x = 0.7, 0.5$  and  $0.3$ ,  $T_c(\infty)$  is taken to be 316 K, 219 K and 128 K,  $C$  is taken to be 1000 K nm, 1300 K nm and 8600 K nm, and  $D_s$  is taken to be 173 nm, 240 nm, and 250 nm respectively. If we define a critical size  $D_{\text{crit}}$  as the size at which  $T_c = 0$  K, then, from the equation,  $D_{\text{crit}} = 176$  nm, 246 nm and 317 nm respectively for  $x = 0.7, 0.5$  and  $0.3$ . Thus the ferroelectric critical size increases with decreasing  $x$ . The samples should be free of defect effect because the sintering temperature is high. Thus one can conclude that size can strongly affect the ferroelectricity.

Figures 3, 4 and 5 show the  $\epsilon'/\epsilon''$  versus  $f$  ( $f$ : 1 MHz  $\sim$  450 MHz) for  $x = 0.7, 0.5$  and  $0.3$ . In Figures 3, 4, and 5,  $\epsilon'$  has a sharp drop with increasing frequency for every sample. In the same frequency range,  $\epsilon''$  shows a peak. Furthermore, an important feature is that the maximum of  $\epsilon''$  shifts to higher frequency as the grain size decreases. For  $x = 0.7$  and  $0.5$ , the  $\epsilon''$  curve is flat for the smallest grain in the measurement frequency region. However,  $\epsilon''$  shows an obvious peak for the smallest grain of  $\text{Ba}_{0.3}\text{Sr}_{0.7}\text{TiO}_3$ . The variations of the relaxation frequency with grain size are shown in Figure 6 for  $x = 0.7, 0.5$  and  $0.3$ . It is seen that the relaxation frequency increases rapidly with decreasing grain size when the grain is small. When grain size is near or larger than  $1 \mu\text{m}$ , the relaxation frequency is independent of the grain size. Furthermore, it is seen that the decrease of  $x$  causes the increase of the relaxation frequency for coarse grained ceramics.

Dielectric dispersion in  $\text{BaTiO}_3$  single crystals as well as ceramics [16] has been observed in the vicinity of the phase transition temperature. The critical slowing down of the relaxation frequency [16], was supposed to be associated with the hopping of off-centre  $\text{Ti}^{4+}$  ions in eight-site potential [4,5]. In  $\text{Ba}_x\text{Sr}_{1-x}\text{TiO}_3$  [16,17], the relaxation process also exhibits critical behaviour in the vicinity of the dielectric peak temperature  $T_c$ . The high-frequency relaxations appear when the temperature is near or above  $T_c$ . Our dielectric measurement showed that the  $T_c$  of  $\text{Ba}_{0.7}\text{Sr}_{0.3}\text{TiO}_3$  samples was near the room temperature,

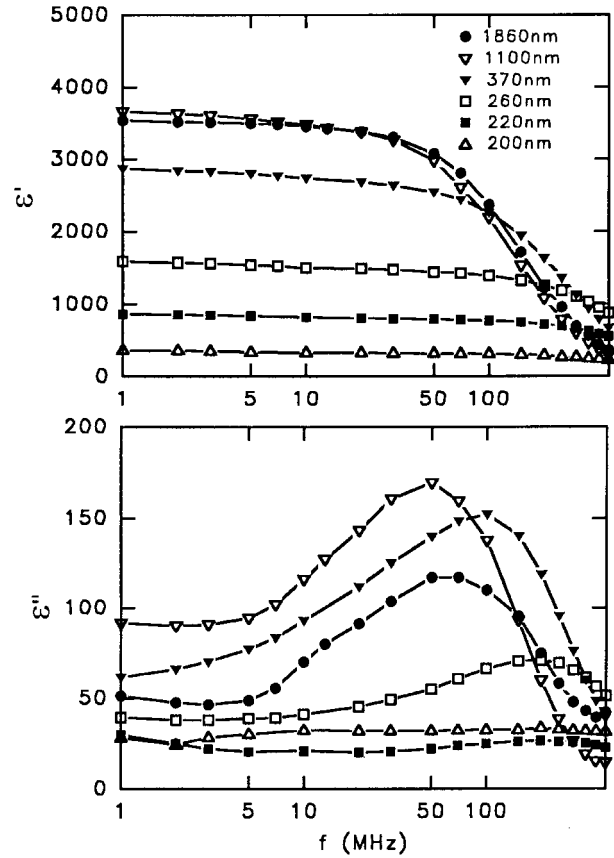


**Fig. 3.** Frequency dependence of  $\epsilon'$  and  $\epsilon''$  for  $\text{Ba}_{0.7}\text{Sr}_{0.3}\text{TiO}_3$  ceramics of different grain size at room temperature.

and those of the samples for  $x = 0.5, 0.3$ , were lower than the room temperature. In addition, the room temperature X-ray diffraction showed that they were all cubic or pseudo-cubic structure. Therefore, the dielectric relaxation in  $\text{Ba}_x\text{Sr}_{1-x}\text{TiO}_3$  can also be explained by means of the above eight-site potential model.

Now we discuss the relation between the relaxation frequency and the grain size according to a double-potential-well model, which is a simplification of the eight-site potential. Figure 7 shows a double-potential-well, where  $h$  is the height of the potential barrier. In the double-potential-well model, the relaxation frequency can be written as:

$$f_r = 2 \frac{w_0}{2\pi} \exp\left(-\frac{h}{kT}\right) \quad (2)$$

where  $w_0/2\pi$  is the oscillation frequency of the Ti ion,  $h$  the height of the potential barrier.

In the discussion of the grain size effect on the room temperature relaxation frequency, the  $T$  and  $w_0$  in equation (2) can be considered as constant. Therefore, we only need to discuss the grain size effect on the height  $h$ . For any calculation, the establishment of a suitable potential function of the double-potential-well is essential. In the molecular-dynamics calculation [18], the following

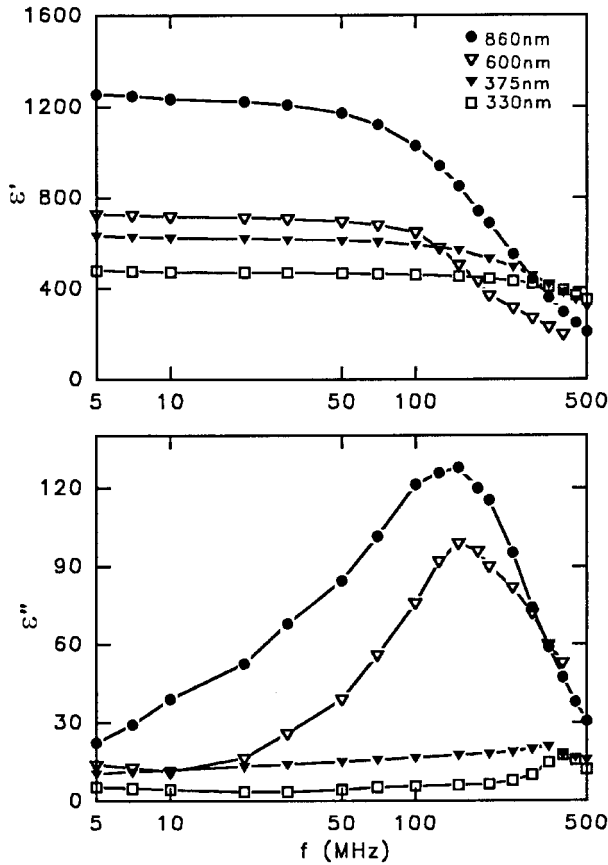


Fig. 4. Frequency dependence of  $\epsilon'$  and  $\epsilon''$  for  $\text{Ba}_{0.5}\text{Sr}_{0.5}\text{TiO}_3$  ceramics of different grain size at room temperature.

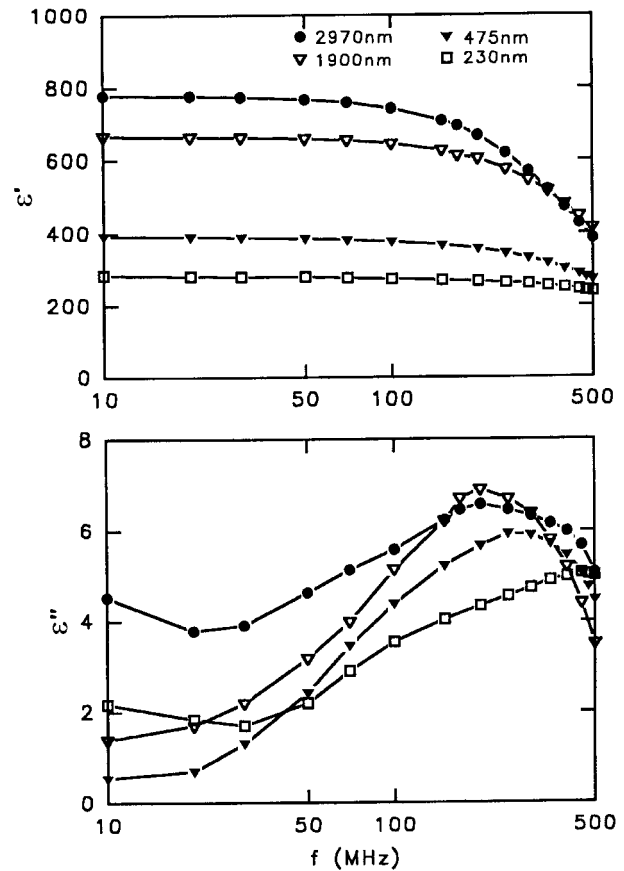


Fig. 5. Frequency dependence of  $\epsilon'$  and  $\epsilon''$  for  $\text{Ba}_{0.3}\text{Sr}_{0.7}\text{TiO}_3$  ceramics of different grain size at room temperature.

pair potential was used:

$$u_{ij} = \frac{Q_i Q_j e^2}{4\pi\epsilon_0 r_{ij}} + f_0(b_i + b_j) \exp\left(\frac{a_i + a_j - r_{ij}}{b_i + b_j}\right) - \frac{C_{ij}}{r_{ij}^6}. \quad (3)$$

This potential consists of an ionic two-body Coulomb interaction (first term), a Born-Mayer-type repulsive interaction (second term), and a van der Waals' attractive interaction (third term).  $Q_i$  and  $Q_j$  are respectively the charges of the  $i$  ion and  $j$  ion, separated by distance  $r_{ij}$ . Furthermore,  $a_i$ ,  $a_j$  and  $b_i$ ,  $b_j$  are potential parameters corresponding to the ionic radius and ionic stiffness, respectively. The parameter  $C_{ij}$  is applied to only oxygen interaction. In equation (3), the Born-Mayer-type repulsive interaction has a negative exponent relation with  $r_{ij}$ . When  $r_{ij} \gg$  the lattice constant, the second term is much lower than the first term. Therefore, the second term and third term will be ignored when we discuss the size effect of the relaxation frequency.

Figure 8 is a spherical crystal grain, its radius is  $R$ . We build an  $X' - Y' - Z'$  coordinate system, the three axes of the system are along the  $[001]$ ,  $[010]$ ,  $[100]$  respectively. We consider a unit cell in the centre of the grain. The centre of the cell is  $(0, 0, 0)$ . We suppose that the sphere

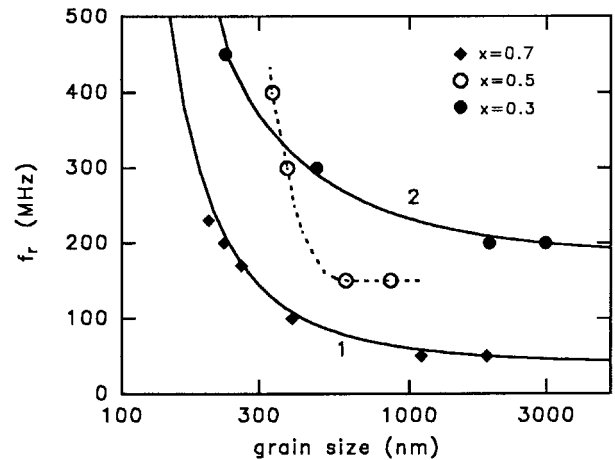


Fig. 6. Grain size dependence of the relaxation frequency for  $\text{Ba}_x\text{Sr}_{1-x}\text{TiO}_3$  ceramics. The dashed line is drawn as a guide to the eye. The solid curves 1 and 2 are the calculation results of  $\text{Ba}_{0.7}\text{Sr}_{0.3}\text{TiO}_3$  and  $\text{Ba}_{0.3}\text{Sr}_{0.7}\text{TiO}_3$  from equation (11).

consists of part 1 and part 2. Part 1 is the inner spheric part with radius  $R'$  ( $R' \gg$  lattice constant).

For the double-potential-well in the centre crystal cell, we suppose that the well is at  $(x, y, z)$ , and the barrier is at  $(x, y, 0)$ ,  $x, y, z \ll R'$ . In Figure 8, when  $R' \rightarrow \infty$ , the internal surface of part 2 can be considered as an equal-potential surface. Therefore, part 2 will not cause any modulation of the electric potential near the sphere centre.

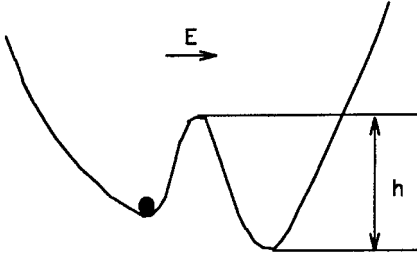


Fig. 7. A double-potential-wells.

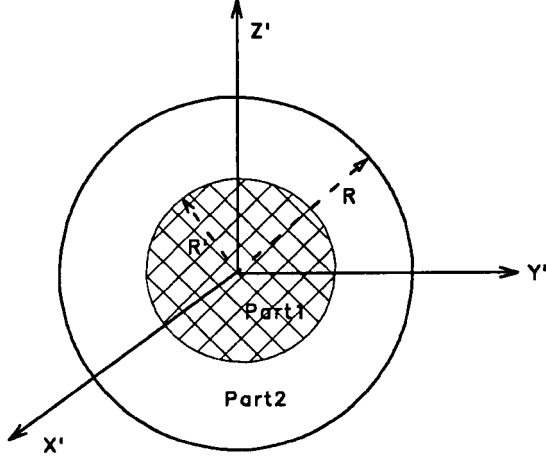


Fig. 8. A crystal grain in  $X' - Y' - Z'$  coordinate system.

With the  $R'$  decreasing, the internal surface of part 2 can not be considered as an equal-potential surface, so part 2 will affect the height  $h$ .

Now we calculate the contribution of part 2 to the electrical potential in paraelectric phase. According to the lattice symmetry of the perovskite structure, part 2 can be divided into the following  $n$  units. In every unit, the positions of the two ions can be written as  $(X, Y, Z)$ ,  $(X, Y, -Z)$ .

Now we calculate the effect of the two ions on the height  $h$ . The potential  $\phi$  at point  $(x, y, 0)$  is:

$$\begin{aligned}\phi &= \frac{QQ(\text{Ti})}{4\pi\epsilon_0} \frac{2}{\sqrt{(X-x)^2 + (Y-y)^2 + Z^2}} \\ &\approx \frac{QQ(\text{Ti})}{4\pi\epsilon_0} 2r \frac{1}{r^2 - Xx - Yy}\end{aligned}$$

where  $r = \sqrt{X^2 + Y^2 + Z^2}$ ,  $Q$  is the charge of the two ions,  $Q(\text{Ti})$  is the charge of the Ti ion at the centre cell.

The potential  $\phi'$  at point  $(x, y, z)$  is:

$$\begin{aligned}\phi' &= \frac{QQ(\text{Ti})}{4\pi\epsilon_0} \left( \frac{1}{\sqrt{(X-x)^2 + (Y-y)^2 + (Z+z)^2}} \right. \\ &\quad \left. + \frac{1}{\sqrt{(X-x)^2 + (Y-y)^2 + (Z-z)^2}} \right) \\ &\approx \frac{QQ(\text{Ti})}{4\pi\epsilon_0} 2r \frac{r^2 - Xx - Yy}{(r^2 - Xx - Yy)^2 - z^2 Z^2}.\end{aligned}$$

Thus the  $\Delta\phi$  of the two ion is:

$$\begin{aligned}\Delta\phi_2 &= \phi - \phi' = \frac{QQ(\text{Ti})}{4\pi\epsilon_0} 2r \frac{-z^2 Z^2}{(r^2 - Xx - Yy)^3} \\ &\approx \frac{QQ(\text{Ti})}{4\pi\epsilon_0} \frac{-2z^2 Z^2}{r^5}.\end{aligned}$$

In a spheric coordinate system:

$$\Delta\phi_2 = -\frac{2}{4\pi\epsilon_0} \frac{QQ(\text{Ti})}{r^3} \cos^2 \theta z^2.$$

Equivalently, the  $\Delta\phi$  of one ion is:

$$\Delta\phi_1 = -\frac{1}{4\pi\epsilon_0} \frac{QQ(\text{Ti})}{r^3} \cos^2 \theta z^2.$$

In the above, the positions of the two ions are  $(X, Y, Z)$ ,  $(X, Y, -Z)$ . An identical result of the  $\Delta\phi_1$  can be obtained if we suppose that the positions are  $(X, Y, Z)$  and  $(-X, Y, Z)$ , or  $(X, Y, Z)$  and  $(X, -Y, Z)$ . For  $\text{Ba}_x\text{Sr}_{1-x}\text{TiO}_3$ , we suppose that the charges of A, B, O ions are  $Q_1$ ,  $Q_2$ ,  $Q_3$  ( $Q_1 + Q_2 + 3Q_3 = 0$ ) respectively. To express the different positions of the three ions, we attach three displacements  $s, t, u$  ( $s, t, u \ll R'$ ) to the  $r$  in  $\Delta\phi$  for A, B, O ions respectively. In the spheric coordinate system, the  $s, t, u$  should be functions of  $\theta$  and  $\varphi$ , but independent of  $r$ . Thus:

$$\begin{aligned}\Delta\phi_A &= -\frac{1}{4\pi\epsilon_0} \frac{Q_1 Q(\text{Ti})}{(r+s)^3} \cos^2 \theta z^2 \\ \Delta\phi_B &= -\frac{1}{4\pi\epsilon_0} \frac{Q_2 Q(\text{Ti})}{(r+t)^3} \cos^2 \theta z^2 \\ \Delta\phi_O &= -\frac{1}{4\pi\epsilon_0} \frac{Q_3 Q(\text{Ti})}{(r+u)^3} \cos^2 \theta z^2.\end{aligned}\quad (4)$$

The  $\Delta\phi$  caused by a crystal cell is:

$$\begin{aligned}\Delta\phi_{\text{cell}} &= \Delta\phi_A + \Delta\phi_B + 3\Delta\phi_O \approx -\frac{Q(\text{Ti})}{4\pi\epsilon_0} \\ &\quad \times \frac{3(Q_2 + 3Q_3)s + 3(Q_1 + 3Q_3)t + 3(Q_1 + Q_2)u}{r^4} \cos^2 \theta z^2.\end{aligned}$$

Therefore, the  $\Delta\phi$  caused by part 2 is:

$$\Delta\phi_{\text{part2}} = \iiint \frac{1}{a^3} \Delta\phi_{\text{cell}} r^2 \sin \theta dr d\theta d\varphi = \beta' \left( \frac{1}{R'} - \frac{1}{R} \right) \quad (5)$$

where  $\beta' = -\iint \frac{Q(\text{Ti})}{4\pi\epsilon_0 a^3} z^2 (3(Q_2 + 3Q_3)s + 3(Q_1 + 3Q_3)t + 3(Q_1 + Q_2)u) \cos^2 \theta \sin \theta d\theta d\varphi$ ,  $a$  is the lattice constant.

According to equation (5), we obtain that the height  $h$  of the potential barrier in the centre of the grain (grain radius =  $R$ ) is:

$$h = h_0 - \frac{\beta'}{R} \quad (6)$$

where  $h_0$  is the height of the potential barrier of a single crystal in the paraelectric phase.

Now we calculate the relation between the height and grain radius in the ferroelectric phase. We suppose that the B ion has a small displacement  $\Delta z$  along  $Z'$  axis in ferroelectric phase. It can be obtained that

$$\begin{aligned}\Delta\phi_A &= -\frac{1}{4\pi\epsilon_0} \frac{Q_1 Q(\text{Ti})}{(r+s)^3} \cos^2 \theta z^2 \\ \Delta\phi_B &= -\frac{1}{4\pi\epsilon_0} \frac{Q_2 Q(\text{Ti})}{(r+t)^3} \cos^2 \theta (z^2 - 2\Delta z z) \\ \Delta\phi_O &= -\frac{1}{4\pi\epsilon_0} \frac{Q_3 Q(\text{Ti})}{(r+u)^3} \cos^2 \theta z^2.\end{aligned}$$

The  $\Delta\phi$  caused by a cell is

$$\begin{aligned}\Delta\phi_{\text{cell}} &\approx \\ &-\frac{Q(\text{Ti})}{4\pi\epsilon_0} \frac{3(Q_2 + 3Q_3)s + 3(Q_1 + 3Q_3)t + 3(Q_1 + Q_2)u}{r^4} \\ &\quad \times \cos^2 \theta z^2 + \frac{Q_2 Q(\text{Ti})}{2\pi\epsilon_0} \frac{1}{r^3} \cos^2 \theta z \Delta z.\end{aligned}$$

Therefore, the  $\Delta\phi$  caused by part 2 is:

$$\Delta\phi_{\text{part2}} = \beta' \left( \frac{1}{R'} - \frac{1}{R} \right) + \lambda$$

$$\lambda = \iiint \frac{1}{a^3} \frac{Q_2 Q(\text{Ti})}{2\pi\epsilon_0} z \Delta z \frac{1}{r} \cos^2 \theta \sin \theta dr d\theta d\varphi.$$

We suppose that the  $\Delta z$  is a constant. It can be obtained that:

$$\lambda = \frac{2}{3} \frac{Q_2 Q(\text{Ti}) z \Delta z}{\epsilon_0 a^3} \ln \frac{R}{R'}.$$

When  $R \rightarrow \infty$ ,  $\ln(R/R') \rightarrow \infty$ . Obviously, the value of  $\Delta\phi_{\text{part2}}$  can not be infinite, otherwise paraelectric phase can not exist. Thus we can deduce that the  $\Delta z$  is not a constant when the grain is in a free state. In fact, the existence of domains can be understood on the basis of qualitative energetic considerations in an ideally perfect ferroelectric crystal. This point is consistent with our deduction.

For a grain with domain structure, the  $\lambda$  can not be integrated. Thus we can not obtain a simple relation between the height  $h$  and radius  $R$ . The grain size of our samples is small. Their Curie temperatures are near or below the room temperature. Therefore, they have a microdomain or cluster structure at room temperature. For a microdomain or cluster, the size is very small, and the structure is unstable. Therefore, the number of crystal cells with a positive  $\Delta z$  equals to that of crystal cells with a negative  $\Delta z$  approximately in any small region of a grain. It can be obtained that  $\lambda \approx 0$  for our samples.

Obviously, the height of the potential barrier will be different at different positions in a grain. It causes that the relaxation frequency has a variation. Thus the relaxation frequency measured in experiments should correspond to the height of some particular position of a grain. Now we calculate the relation between the grain radius  $R$  and the height  $h$  of the particular position in paraelectric phase.

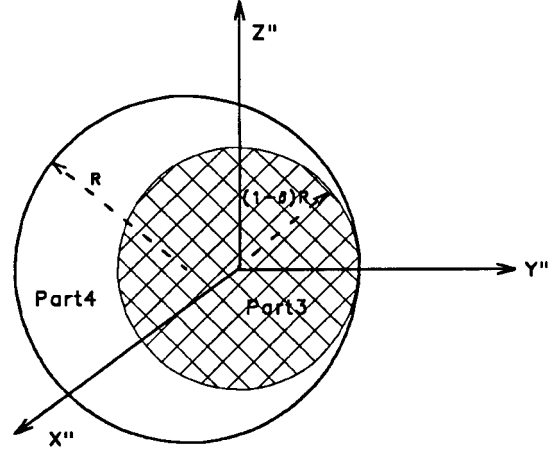


Fig. 9. A crystal grain in  $X'' - Y'' - Z''$  coordinate system.

In Figure 8, we suppose that the particular position is at  $(0, 0, \delta R)$ ,  $0 \leq \delta \leq 1$ . We build an  $X'' - Y'' - Z''$  coordinate system at  $(0, 0, \delta R)$ , the three axes of the system are along the  $X', Y', Z'$  respectively. Now we observe the sphere and the  $X'' - Y'' - Z''$  coordinate system in Figure 9. We suppose that the sphere consists of part 3 and part 4. Part 3 is the inner spheric part with radius  $(1 - \delta)R$ . Its centre is at the origin of the  $X'' - Y'' - Z''$  system. Therefore, the height  $h$  at the origin of the coordinate system is:

$$h = \Delta\phi_{\text{part3}} + \Delta\phi_{\text{part4}}. \quad (7)$$

The  $\Delta\phi_{\text{part3}}$  and  $\Delta\phi_{\text{part4}}$  are the  $\Delta\phi$  caused by part 3 and part 4 respectively.

According to equation (6), it can be obtained

$$\Delta\phi_{\text{part3}} = h_0 - \frac{\beta'}{(1 - \delta)R}. \quad (8)$$

In addition,

$$\Delta\phi_{\text{part4}} = \iiint_{\text{part4}} \frac{1}{a^3} \Delta\phi_{\text{cell}} dV.$$

In a spheric coordinate system

$$dV = S dr = \frac{\pi r(2\delta R r - r^2 + (1 - \delta^2)R^2)}{\delta R} dr.$$

Therefore,

$$\Delta\phi_{\text{part4}} = \frac{\beta''}{R}. \quad (9)$$

$$\beta'' = \left( \frac{-2-4\delta}{1-\delta^2} + \frac{1}{\delta} \ln \frac{1+\delta}{1-\delta} \right) \iint \frac{Q(\text{Ti})}{4\epsilon_0 a^3} z^2 (3(Q_2 + 3Q_3)s + 3(Q_1 + 3Q_3)t + 3(Q_1 + Q_2)u) \cos^2 \theta d\theta d\varphi.$$

According to equations (7-9), it can be obtained

$$h = h_0 - \frac{\beta}{R} \quad (10)$$

$$\beta = (\beta' - (1 - \delta)\beta'')/(1 - \delta).$$

According to equations (2, 10), the relaxation frequency  $f_r$  is:

$$f_r = \frac{w_0}{\pi} \exp\left(-\frac{h}{kT}\right) = f_{r0} \exp\left(\frac{\gamma}{R}\right) \quad (11)$$

where the  $f_{r0}$  is the relaxation frequency of single crystal,  $f_{r0} = (w_0/\pi) \exp(-\frac{h_0}{kT})$ ,  $\gamma = \beta/kT$ .

In equations (10, 11),  $\beta/R$  and  $\gamma/R$  are zero approximately when  $R$  is large. Thus the height  $h$  and relaxation frequency  $f_r$  are grain size independent in coarse grained ceramics. Now we suppose that the  $R$  is small. According to equations (10, 11), the change of the height  $h$  and relaxation frequency  $f_r$  should be more and more quick with  $R$  decreasing. Obviously, these results are consistent with the experimental phenomena. In Figure 6, the relaxation frequency increases with grain size decreasing. Therefore, the  $\gamma$  should be a positive value in equation (11). Now we suppose that the  $Q_1, Q_2, Q_3, Q(\text{Ti})$  are +2, +4, -2, +4 respectively, the  $s, t, u$  are constant, the  $\delta$  is 0. Thus we obtain

$$\gamma = \beta/kT = \frac{-8z^2}{kT\epsilon_0 a^3} (3u - 2t - s).$$

So we deduce  $3u - 2t - s < 0$  from the experimental result and above equation. Now we observe the distances between the Ti ion in the centre cell and its neighboring A, B, O ions. The distance between the Ti ion and O ion is the smallest. The distance between the Ti ion and B ion is the largest. Therefore, we can obtain  $u < s < t$  for the neighboring ions of the Ti ion of the centre cell. Obviously, it can be extended to equation (4). Thus we obtain  $3u - 2t - s < 0$  and  $\gamma > 0$ . It is consistent with the above deduction from the experimental result. Furthermore, the height  $h$  should decrease with grain size decreasing due to  $3u - 2t - s < 0$ .

We adjust the  $f_{r0}$  and  $\gamma$  of equation (11), and get theoretical curves. Figure 6 shows the theoretical curves for  $x = 0.7$  and  $0.3$ . They both are in good agreement with the experimental result. The  $f_{r0}$  and  $\gamma$  are 39.5 MHz and 180 nm for  $x = 0.7$ , 183 MHz and 105 nm for  $x = 0.3$ . It is a pity that the experimental result of the  $\text{Ba}_{0.5}\text{Sr}_{0.5}\text{TiO}_3$  ceramics has a deviation from equation (11). When the grain size decreases from the bulk size to the ferroelectric critical size, the change  $\Delta h$  of the barrier height is

$$\Delta h = \frac{2\beta}{D_{\text{crit}}} = \frac{2\gamma kT_r}{D_{\text{crit}}} \quad (12)$$

where  $T_r$  is the room temperature. The calculation shows that the  $\Delta h$  for  $x = 0.7$  and  $0.3$  are 0.0529 eV and 0.0171 eV respectively. The former is much higher than the latter. It gives an approximate explanation on the fact that the bulk Curie temperature of  $\text{Ba}_{0.7}\text{Sr}_{0.3}\text{TiO}_3$  is higher than that of  $\text{Ba}_{0.3}\text{Sr}_{0.7}\text{TiO}_3$  obviously.

In the above model, the crystal lattice is supposed to be in perfect order. In real ceramics, macroscopic stresses between the grains and in the grains will causes a random distortion of the lattice. The distortion will decrease the symmetry of the lattice, and decrease the effect of the

long-range Coulomb potential. Thus the random stresses tend to decrease the height  $h$  and suppress the ferroelectricity. In our previous work, some  $\text{BaTiO}_3$  samples prepared by the sol-gel method were chosen to make a high-resolution transmission electron microscopic study [19]. The study shows that their lattice is in perfect order. It means that the effect of the stress is faint in our samples. The porosity of ceramics is a considerable problem. The air can not influence the relaxation measurement. However, the decrease of the porosity means that the Coulomb potential caused by a grain could influence the dielectric behaviors of its neighboring grains. The direction of a grain in ceramics is arbitrary. It means that the interaction among grains can not change the height  $h$  and the relaxation frequency  $f_r$  obviously. However, the interaction among grains could change the dielectric constant. When an electric field is applied to the ceramics, every grain is polarized by the applied field. The polarization locally modifies the applied field in the surrounding air. It means the change of the dielectric constant. When only small volume fraction of grains is present the influence among grains, is negligible and so the prediction of the potential by using the isolated grain model is physical reasonable. The porosity of our sol-gel derived samples is high. It is advantageous to use the isolated grain model.

According to our experimental results and above discussion, we can draw the following conclusions. The height  $h$  in the centre of coarse grained ceramics is grain size independent, while for fine grained ceramics, the height  $h$  is more and more quickly decreased with grain size decreasing. The decrease of the height  $h$  will facilitate the hopping of Ti ion among the potential wells. It will lead to a reduction and suppression of possible ferroelectricity. According to the change of the height  $h$  with grain size, it is easy to understand the fact that the ferroelectricity in coarse grained ceramics is similar to that of single crystal, while ferroelectricity of fine grained ceramics is suppressed rapidly with grain size decreasing.

An analogy can be drawn among ferroelectric phase transitions in nanocrystals, the magnetic phase transitions in nanocrystals [20–22] and other solid-solid phase transitions in nanocrystals [23]. Magnetic nanocrystals behave as single domains, which at high temperatures are superparamagnetic and respond to an applied field with no hysteresis. As the system is cooled below the “blocking temperature”, the magnetization *versus* applied field shows hysteresis, including remanence (residual magnetization after the applied field is turned off). The characteristic relaxation time for this hysteresis follows the simple equation

$$\tau_{1/2} \propto \exp\left(\frac{KV}{k_B T}\right) + \text{surface term}$$

where  $K$  is the crystalline anisotropy and  $V$  the volume of the crystal [24, 25]. In crystals above a certain size, multiple magnetic domains are observed, and this equation no longer applies. Furthermore, the size dependence of structural metastability in semiconductor nanocrystal system CdSe was observed by Chen *et al.* [23]. Barrier heights

were observed to increase with increasing nanocrystal size. In ferroelectric phase transitions, nanocrystals below a certain size behaves as single structural domains, and the kinetic barrier “blocking” the transition can cause the system to be metastable. These results all suggest that general rules may be of use in the explanation of new metastable phases in a solid.

In Figure 6, it seems that the relaxation frequency increases with  $x$  decreasing at least when the grain size is near and larger than  $1 \mu\text{m}$ . It is easily understandable if we take into account the facts that the critical slowing down of the relaxation exists in  $\text{Ba}_x\text{Sr}_{1-x}\text{TiO}_3$ , that the  $T_c$  of  $\text{Ba}_x\text{Sr}_{1-x}\text{TiO}_3$  decreases with  $x$  decreasing, and that the dielectric measurement was carried out at room temperature for all the samples with different  $x$ . This phenomenon can further be discussed according to equation (3). In equation (3), the second term is a repulsive interaction. It can make the Ti ion stay at the centre of a cell. In fact, the Ti ion does not stay at the centre. Thus we can deduce that the displacement of Ti ion should be attributed to the Coulomb interaction. For  $\text{BaTiO}_3$ , the cell size decreases when Sr ion substitutes the Ba ion. Therefore, the  $r_{ij}$  in equation (3) has a decrease. According to equation (3), the decrease of  $r_{ij}$  can increase both the Coulomb interaction and the repulsive interaction. Since the increase of the repulsive interaction is larger than that of the Coulomb interaction, the deviation of the Ti ion from the centre of the crystal cell will decrease. With the tendency continuing, the repulsive interaction will make the Ti ion go to the centre of the crystal cell in the end. Thus the height  $h$  is 0. In reference [18], the molecular-dynamics calculation showed that the calculated  $\text{SrTiO}_3$  structure was cubic. Thus it can be obtained that the height  $h$  in  $\text{SrTiO}_3$  is zero. For  $\text{Ba}_x\text{Sr}_{1-x}\text{TiO}_3$ , if the change of the  $h$  is monotonic with  $x$  changing from 1 to 0, we can obtain the conclusion that the  $h$  decreases with  $x$  decreasing. The conclusion can be proved by the cell effect of  $\text{Ba}_x\text{Sr}_{1-x}\text{TiO}_3$  indirectly [9,10]. In our previous work [9,10], it is argued that the variation of the ferroelectricity in  $\text{Ba}_x\text{Sr}_{1-x}\text{TiO}_3$  is determined by a change in the cell volume whether the change is produced by a change in pressure or a change in composition. In  $\text{BaTiO}_3$ , the relation among the cell volume, the barrier height, and the ferroelectricity has been proved by Cohen *et al.* [1]. Thus the decrease of  $x$  for  $\text{Ba}_x\text{Sr}_{1-x}\text{TiO}_3$  causes the decrease of the cell volume and the barrier height. The oscillation frequency ( $w_0/2\pi$ ) should have an increase because of the decrease of the cell volume. According to equation (2) and the above two factors, we can obtain the conclusion that the relaxation frequency increases with decreasing  $x$ .

For the  $\text{Ba}_x\text{Sr}_{1-x}\text{TiO}_3$  samples, we found that the diffusion of their dielectric peaks gave some useful information. Figure 10 shows the relation between the  $f_r$  and the temperature width  $\Delta T$  at 75% of  $\epsilon_{\text{max}}$  ( $\Delta T = T_{0.75\epsilon(\text{max})} - T_{\epsilon(\text{max})}$  for  $T_{0.75\epsilon(\text{max})} > T_{\epsilon(\text{max})}$ ) for  $x = 0.7, 0.5, 0.3$ . For  $\text{Ba}_x\text{Sr}_{1-x}\text{TiO}_3$ , we think that the increase of the  $\Delta T$  reflects the suppression of the ferroelectricity. In Figure 10, it seems that the  $\Delta T$  is corresponding with the  $f_r$  for different samples. For  $\text{Ba}_x\text{Sr}_{1-x}\text{TiO}_3$ , the change of

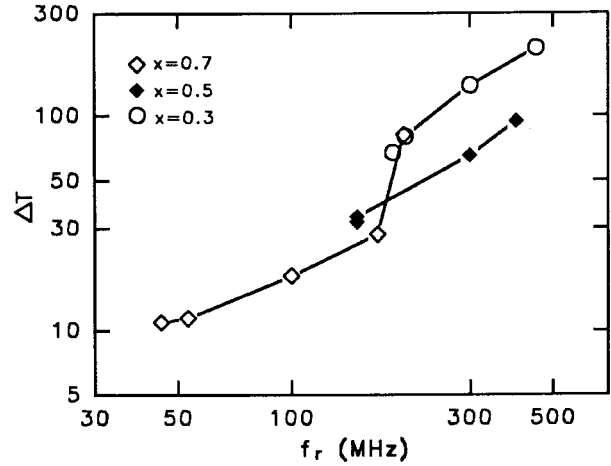


Fig. 10. Relation between the relaxation frequency and  $\Delta T$  for  $\text{Ba}_x\text{Sr}_{1-x}\text{TiO}_3$  ceramics.

the lattice constant is only about 1% when  $x$  changes from 0.7 to 0.3. Thus the change of the oscillation frequency in equation (2) is very small. According to equation (2) and Figure 10, it seems that the ferroelectricity is corresponding with the height  $h$  for  $\text{Ba}_x\text{Sr}_{1-x}\text{TiO}_3$  ceramics. Thus the existence of a multi-site potential structure (the height  $h > 0$ ) is a prerequisite for the existence of the ferroelectricity of  $\text{Ba}_x\text{Sr}_{1-x}\text{TiO}_3$  ceramics.

According to our work, the anisotropy of the dielectric constants in perovskite structure can be explained by the eight-site potential model. As reported by reference [26], the  $\epsilon_c$  and  $\epsilon_a$  of  $\text{BaTiO}_3$  single-domain crystals are 200 and 4000 respectively at room temperature. In the tetragonal phase, the Ti ions preferentially occupy four of the eight sites, giving a net polarization along  $c$ -axis. Therefore, an electric field along  $a$ -axis can cause an additional hopping of Ti ions in four sites. It results in a greater dielectric constant  $\epsilon_a$ . An electric field along  $c$ -axis can not cause such an additional hopping. Thus the  $\epsilon_c$  is much smaller.

## 4 Summary

For  $\text{Ba}_x\text{Sr}_{1-x}\text{TiO}_3$  system, the transition temperature  $T_c$  decreases and the transition becomes diffuse as the grain size decreases. Our experiments and model have evidenced a size dependence of relaxation frequencies and barrier heights at room temperature for  $\text{Ba}_x\text{Sr}_{1-x}\text{TiO}_3$  with  $x = 0.7, 0.5, 0.3$ . The relaxation frequency  $f_r$  increases rapidly with grain size decreasing for fine grained ceramics, and it is independent of the grain size for coarse grained ceramics. Our model explains the fact that the grain size affects the barrier height and therefore changes the relaxation characteristics and the structural metastability. For  $x = 0.7, 0.3$ , this model is in quantitative agreement with the experimental results. The decrease of  $x$  causes the decrease of the barrier height, and the increase of the relaxation frequency. The appearance of ferroelectricity and anisotropy of the dielectric constant have an intimate relation with the barrier height of the eight-site



potential. It seems that the kinetics of ferroelectric phases can be understood more clearly in nanocrystals according to the potential distribution.

This work was supported by a grant for State Key Program for Basic Research of China, and the research fund for the doctoral program of higher education.

## References

1. R.E. Cohen, H. Krakauer, *Phys. Rev. B* **42**, 6416 (1990).
2. R.E. Cohen, *Nature* **353**, 136 (1992).
3. D.L. Decker, Y.X. Zhao, *Phys. Rev. B* **39**, 2432 (1989).
4. R. Comes, M. Lambert, A. Guinier, *Solid State Commun.* **6**, 715 (1968).
5. K. Itoh, L.Z. Zeng, E. Nakamura, N. Mishima, *Ferroelectrics* **63**, 29 (1985).
6. D. Turnbull, *J. Chem. Phys.* **40**, 411 (1952).
7. D. Turnbull, *Solid State Phys.* **3**, 225 (1956).
8. V.V. Lemanov, E.P. Smirnova, P.P. Syrnikov, E.A. Tarakanov, *Phys. Rev. B* **54**, 3151 (1996).
9. L. Zhang, W.L. Zhong, Y.G. Wang, P.L. Zhang, *Solid State Commun.* **104**, 263 (1997).
10. L. Zhang, W.L. Zhong, Y.G. Wang, C.L. Wang, P.L. Zhang (to be published).
11. W.L. Zhong, P.L. Zhang, Y.G. Wang, T.L. Ren, *Ferroelectrics* **160**, 55 (1994).
12. R. Landauer, *J. Appl. Phys.* **23**, 779 (1952).
13. K. Uchino, E. Sadanaga, T. Hirose, *J. Am. Ceram. Soc.* **72**, 1555 (1989).
14. K. Ishikawa, K. Yoshikawa, N. Okada, *Phys. Rev. B* **37**, 5852 (1988).
15. W.L. Zhong, B. Jiang, P.L. Zhang, J.M. Ma *et al.*, *J. Phys.-Cond.* **5**, 2619 (1993).
16. S. Kazaoni, J. Ravez, C. Elissalde, M. Maglione, *Ferroelectrics* **135**, 85 (1992).
17. N. Singh, D. Pandey, *J. Phys.-Cond.* **8**, 4269 (1996).
18. H. Tanaka, H. Tabata, K. Ota, T. Kawai, *Phys. Rev. B* **53**, 14112 (1996).
19. L.A. Bursill, B. Jiang, J.L. Peng *et al.*, *Ferroelectrics* **191**, 281 (1997).
20. E.C. Stoner, E.P. Wohlfarth, *Philos. Trans. R. Soc. London Ser. A* **240**, 599 (1948).
21. L. Neel, *Ann. Geophys.* **5**, 99 (1949).
22. D.D. Awschalom, D.P. Divincenzo, *Phys. Today* **48**, 43 (1995).
23. C.C. Chen, A.B. Herhold, C.S. Johnson, A.P. Alivisatos, *Science* **276**, 398 (1997).
24. F. Bodker, S. Morup, S. Linderoth, *Phys. Rev. Lett.* **72**, 282 (1994).
25. J.P. Chen, C.M. Sorensen, K.J. Klabunde, G.C. Hadjipanayis, *Phys. Rev. B* **51**, 11527 (1995).
26. W.J. Merz, *Phys. Rev.* **76**, 1221 (1949).